Quaternion-Optimization-Based In-Flight Alignment Approach for Airborne POS

Kang Taizhong, Fang Jiancheng, and Wang Wei

***Abstract*—Position and Orientation System (POS) is a key technology that provides motion compensation information for imaging sensor in airborne remote sensing. In-flight alignment (IFA) is an important alignment method that can improve reaction speed and accuracy of measurement for airborne POS. The traditional IFA methods based on the Kalman filter and the adaptive extended Kalman filter (AEKF) are severely affected by flight maneuver; severe maneuver may result in alignment accuracy degeneration or failure. On the basis of optimization-based alignment method for static base alignment, a novel IFA method based on quaternion optimization is devised in this paper, aiming to boost up the robustness and the accuracy of IFA, which extends the range of the application of optimization-based alignment method from static base alignment to IFA. The proposed algorithm has the advantage that it can avoid the affection from severe maneuver. The real-time implementation is given. Flight experiment demonstrates that, compared with the IFA method based on AEKF, the proposed algorithm is better in converging speed and robusticity with the same alignment accuracy.**

***Index Terms*—Flight maneuver, in-flight alignment (IFA), Position and Orientation System (POS), quaternion-constrained least square, robust, Strapdown Inertial Navigation System (SINS)/Global Positioning System (GPS) integrated navigation system.**

I. Introduction

THE POSITION and Orientation System (POS) is a key technology in the field of airborne direct georeferencing which is widely used to compensate the motion error for various airborne imaging load camera, Synthetic Aperture Radar (SAR), InSAR, etc. [1]. In-flight alignment (IFA) is an important function in POS, with which some urgent missions can be accomplished, e.g., natural disaster rescue, military mission, etc. In addition, it works for some special missions, in which ground static base alignment cannot be implemented. Therefore, IFA is an important substitution of ground static base alignment [1], [2].

In the process of IFA, generally, the initial position and velocity are directly acquired from the Global Positioning System (GPS). Therefore, IFA essentially indicates the attitude alignment. In contrast to ground static base alignment, the IFA process is often in the circumstance of maneuver in air, which enormously increases the difficulty to implement attitude alignment [2].

The existing IFA method generally consists of two steps; the first step is coarse alignment, which get the initial level attitude with accelerometer outputs from the inertial measure unit (IMU) and get the heading angle with GPS heading information. The second step is fine alignment, which generally takes the velocity and the position error as measurement from Strapdown Inertial Navigation System (SINS) and GPS into a Kalman filter to estimate the attitude error gradually and feed back to amend the attitude [1], [2]. However, the aforementioned scheme has several shortcomings as follows: 1) The flight maneuver and the drift angle may result in large level attitude and heading attitude error, and may bring system nonlinearity into the fine alignment. 2) In the fine alignment, acute maneuver is involved to boost up the system observable degree [3], in which more acute maneuver can help make the attitude converge faster, but meanwhile, acute maneuver can bring other error factors, which cannot be ignored, such as volatile lever arm error, size effect of IMU, and other errors caused by libration, so as to bring severe system module uncertainty and make the filtering nonoptimal and unstable [4].

To solve the problem of system nonlinearity, several nonlinear filter methods are commonly used. The predictive iterated Kalman filter is successfully applied in the Inertial Navigation System (INS)/GPS integration [5]. Several nonlinear Kalman filters in POS are analyzed and compared [6]. Nonlinear filtering methods are used in the INS alignment [7]. An extended Kalman filter (EKF) based leveling method is used for an underwater vehicle [8]. Nonsymmetric unscented transformation is used in IFA [9]. The predictive Kalman filter is used in the INS nonlinear alignment under large azimuth misalignment angle [10]. The INS navigation alignment method is used in in-drilling alignment [11]. Tightly coupling IMU/radio-frequency-identification integration is used in accurate pedestrian indoor navigation [12]. Observability analysis is implemented for the INS alignment in horizontal drilling [13]. Artificial-neural-network methods are used in multisensor integration [14]. Among them, the large quantity of calculation in unscented Kalman filter, particle filter, and marginalized particle filter limits their application in practice [7],

Manuscript received January 16, 2012; revised April 10, 2012; accepted April 30, 2012. Date of publication July 20, 2012; date of current version October 10, 2012. This paper was supported in part by the National Basic Research Program of China under Grant 2009CB724002, by the National Basic Research Program of China under Grant 2009CB724001, by China National Funds for Distinguished Young Scientists under Grant 60825305, by the Foundation for Innovative Research Groups of the National Natural Science Foundation of China under Grant 61121003, by the National Natural Science Foundation of China under Grant 61004129, and by the National Natural Science Foundation of China under Grant 60904093. The Associate Editor coordinating the review process for this paper was Dr. G. Xiao.

The authors are with the "Inertial Technology" Key Laboratory, Beijing University of Aeronautics and Astronautics, Beijing 100191, China (e-mail: kangtaizhong@aspe.buaa.edu.cn; fangjiancheng@buaa.edu.cn).

The authors contributed equally to this paper.

Color versions of one or more of the figures in this paper are available online at http://ieeexplore.ieee.org.

Digital Object Identifier 10.1109/TIM.2012.2202989

[15]–[17]. The EKF is the most widely used method for its good real-time performance, but it depends on the prior knowledge on the accuracy of coarse alignment and the measurement noise; meanwhile, the instability of the GPS measurement error can lead to severe estimation error. To solve this problem, a new IFA method on the innovation adaptive EKF (AEKF) for airborne POS is proposed [2], which introduces the calculated innovation covariance into the computation of filter gain matrix directly, so that the system error caused by unstable GPS measurement is eliminated. However, this method cannot get rid of the dependence on the initial standard deviation matrix of initial attitude and is not robust enough in the circumstance of large initial heading error.

Other than Kalman-filter-related methods, an innovation static alignment method is contributed, in which the static alignment problem is transformed into the optimization problem [18], [19] with the equivalent q-method of the Wahba problem [20]. The results of this paper suggest a new avenue for inertial navigation alignment research. However, due to the precondition of zero acceleration in all three directions, this method can be only used in static circumstance or swaying circumstance without linear acceleration in any direction [18]–[25]. Essentially, the equivalent q-method to the Wahba problem is a constrained least-square attitude determination method.

On the basis of the alignment method devised by Yuanxin, a new IFA method is devised in this paper, which follows the ideology of Yuanxin's aforementioned method, and transforms the IFA problem into an optimization problem of finding the minimum eigenvalue in the form of quaternion. Absolutely different from traditional Kalman filter method, the proposed algorithm is an innovative way that has never been explored to solve the IFA problem. In contrast with the traditional Kalman filter method, the proposed algorithm has prominent advantages in aspects as follows: First, the proposed algorithm is completely analytic without any initial information uncertainty, in which no probability estimation is involved. Second, there is no linearization simplification in the proposed algorithm as no nonlinear factor exists. Therefore, the alignment process does not rely on the maneuver and is fit for any circumstance with any acute motions; in other words, it is robust enough against motion disturbance.

Then, the real-time implementation is given. Finally, experiment is carried out to validate the effectivity, the accuracy, and the robustness of the proposed algorithm in this paper.

The rest of this paper is organized as follows. Section II presents the proposed quaternion-optimization-based IFA mathematical model and algorithm. Section III improves the proposed algorithm into real-time application. Finally, experiment is carried out in Section IV, and conclusion is presented in Section V.

II. Mathematical Modeling and Algorithm

In the conventional inertial navigation theory, the track of SINS navigation drifts away from the true motion track (the GPS information can be treated as the "true motion track" on a certain extent). Just as Fig. 1 shows, with true initial attitude and tiny IMU error, the flight track calculated by airborne SINS can go across the GPS track, and with "wrong initial attitude," the SINS track goes far away from the GPS track gradually (Here, "track" can be understood as any navigation parameter curves, such as velocity curve and attitude curve).

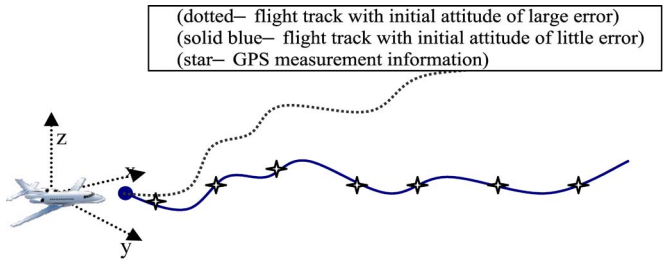

Fig. 1. Sketch map (SINS navigation track with different initial attitudes).

Based on the aforementioned analysis, the true initial value can be calculated by some way, so as to make the SINS track across the true motion track by some particular rules.

To solve this problem, it is necessary to start from the analysis of the classical SINS navigation algorithm.

In the conventional SINS process, the local level frame is often selected as the navigation reference frame. In this frame, the attitude differential equation of the IMU is [18]

$$\dot{C}_b^n = C_b^n \left(\omega_{nb}^b \times\right), \omega_{nb}^b = \omega_{ib}^b - C_n^b \left(\omega_{ie}^n + \omega_{en}^n\right) \tag{1}$$

where the notations of b, n, i, and e denote different reference frames (particular description in Appendix), and C_b^n is the attitude matrix, which is updated by the angular rate of the body frame ω_{nb}^b with respect to the navigation frame. $(\omega_{nb}^b \times)$ denotes the cross-product operator of ω_{nb}^b, which can be expressed as $\left(\omega_{nb}^b \times\right) = \begin{pmatrix} 0[[[fd]]] & -\omega_{nbz}^b[[[fd]]] & \omega_{nby}^b \\ \omega_{nbz}^b[[[fd]]] & 0[[[fd]]] & -\omega_{nbx}^b \\ -\omega_{nby}^b[[[fd]]] & \omega_{nbx}^b[[[fd]]] & 0 \end{pmatrix}$. ω_{nb}^b is composed of the following three parts: ω_{ib}^b denotes the angular rate of the body frame with respect to the inertial frame, which is directly measured by the three gyros of the IMU; ω_{ie}^n is the earth rotation rate vector in the navigation frame; and ω_{en}^n is the navigation frame angular rate in the earth frame.

The velocity differential equation of the body frame is

$$\dot{v}_{en}^n = C_b^n f^b + G^n - \left(2\omega_{ie}^n + \omega_{en}^n\right) \times v_{en}^n - \omega_{ie}^n \times \left(\omega_{ie}^n \times R^n\right) \tag{2}$$

where v_{en}^n denotes the velocity of the navigation frame with respect to the earth frame, f^b is the specific force directly measured by the IMU in the body frame, G^n denotes the centrifugal force, and R^n denotes the radius of the earth.

The earth gravity is comprised of

$$\overline{g} = \overline{G} - \overline{\omega}_{ie} \times \left(\overline{\omega}_{ie} \times \overline{R}\right). \tag{3}$$

in which $\overline{G}$ denotes the centrifugal force, $\overline{\omega}_{ie}$ denotes the earth rotation, and $\overline{R}$ denotes radius of the earth.

Equation (2) can be rewritten as

$$\dot{v}_{en}^n = C_b^n f^b - \left(2\omega_{ie}^n + \omega_{en}^n\right) \times v_{en}^n + g^n. \tag{4}$$

The steps in the strapdown can be summarized in Fig. 2. In the navigation frame, the attitude differential equation is

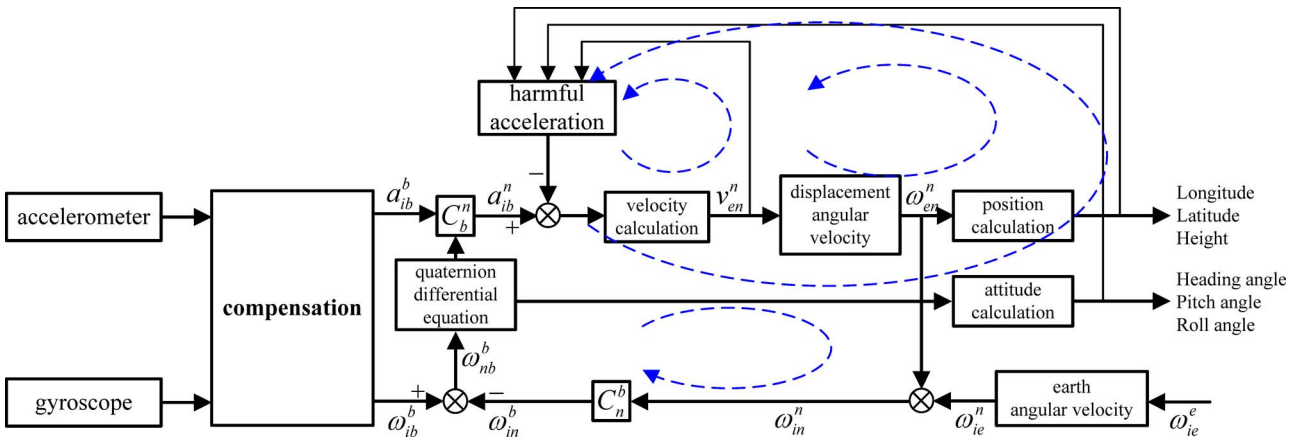

Fig. 2. Signal flow graph (strapdown navigation flow with feedback circle).

updated with the attitude, the velocity, and the position feedback, as shown in Fig. 2, in which the relationship is nonlinear between attitude $C_b^n(t)$ and the initial attitude $C_b^n(0)$; accordingly, it is hard to create a resolution relationship between velocity v_{en}^n and the initial attitude $C_b^n(0)$.

In Fig. 2, after compensation, the original signals of the gyroscopes and the accelerometers are transformed into the angular velocity ω_{ib}^b and acceleration a_{ib}^b; harmful acceleration denotes terms $(2\omega_{ie}^n + \omega_{en}^n) \times v_{en}^n - g^n$ in (4), and the other items in Fig. 2 are consistent with the classical angle and velocity updating method in the SINS theory.

In hopes of getting a resolution relationship between $C_b^n(t)$ and $C_b^n(0)$, obviously, the feedback circle is the main obstacle. To remove the feedback circle, reconsider this problem in the inertial frame; the attitude differential equation is

$$\dot{C}_b^i = C_b^i \left(\omega_{ib}^b \times\right) \tag{5}$$

where C_b^i is the attitude matrix of the body frame with respect to the inertial frame, which is updated by ω_{ib}^b, which denotes the angular rate of the body frame with respect to the inertial frame, and ω_{ib}^b is directly measured by IMU; the relationship between $C_b^i(t)$ and $C_b^i(0)$ is

$$C_b^i(t) = \chi(0,t) C_b^i(0). \tag{6}$$

The prominent advantage of (6) is that $\chi(0,t)$ has no relationship with $C_b^i(0)$ and $\chi(0,t)$ is retrieved from ω_{ib}^b alone.

Meanwhile, the velocity differential equation is expressed in the inertial frame as

$$\dot{v}_{en}^i = f^i - \left(2\omega_{ie}^i + \omega_{en}^i\right) \times v_{en}^i + g^i. \tag{7}$$

Expand (7) as

$$\dot{v}_{en}^i = C_b^i f^b - \left(2C_n^i \omega_{ie}^n + C_n^i \omega_{en}^n\right) \times C_n^i v_{en}^n + C_n^i g^n. \tag{8}$$

From (8), v_{en}^i is retrieved as

$$v_{en}^i = C_n^i v_{en}^n = C_b^i(0) \int \chi(0,t)^T f^b dt - \int C_n^i \left(\left(2C_i^n \omega_{ie}^i + \omega_{en}^n\right) \times v_{en}^n + g^n\right) dt. \tag{9}$$

Reorganize the aforementioned formula as

$$C_n^i v_{en}^n + \int C_n^i \left(\left(2C_i^n \omega_{ie}^i + \omega_{en}^n\right) \times v_{en}^n + g^n\right) dt = C_b^i(0) \int \chi(0,t)^T f^b dt.$$

Change for another expression as

$$\beta(t) = C_b^i(0) \alpha(t) \tag{10}$$

where $\beta(t)$ and $\alpha(t)$ are given as

$$\beta(t) = \left(C_n^i(t) v_{en}^n(t) - C_n^i(0) v_{en}^n(0)\right) + \int_0^t C_n^i(\tau) \left(\left(2C_i^n(\tau) \omega_{ie}^i + \omega_{en}^n(\tau)\right) v_{en}^n(\tau) + g^n\right) d\tau \tag{11}$$

$$\alpha(t) = \int_0^t \chi(0,t)^T f^b(\tau) d\tau. \tag{12}$$

In expression $\alpha(t)$, there are only measurement quantities from IMU, i.e., angular rate and acceleration. In expression $\beta(t)$, all the variables can be directly acquired or substituted by the GPS information. That makes it possible to get the parse resolution of the initial attitude.

In the expression $\beta(t)$, for the sake of convenience, define the earth frame at the initial time to be the inertial frame, and consequently

$$\begin{aligned} C_n^i(t) &= C_e^i(t) C_n^e(t) \\ &= \begin{bmatrix} \cos\left(\omega_{ie}^n t\right) & \sin\left(\omega_{ie}^n t\right) & 0 \\ -\sin\left(\omega_{ie}^n t\right) & \cos\left(\omega_{ie}^n t\right) & 0 \\ 0 & 0 & 1 \end{bmatrix} \\ &\quad \cdot \begin{bmatrix} -\sin(\lambda(t)) & -\sin(L(t)) \cdot \cos(\lambda(t)) & \cos(L(t)) \cdot \cos(\lambda(t)) \\ \cos(\lambda(t)) & -\sin(L(t)) \cdot \sin(\lambda(t)) & \cos(L(t)) \cdot \sin(\lambda(t)) \\ 0 & \cos(L(t)) & \sin(L(t)) \end{bmatrix} \end{aligned} \tag{13}$$

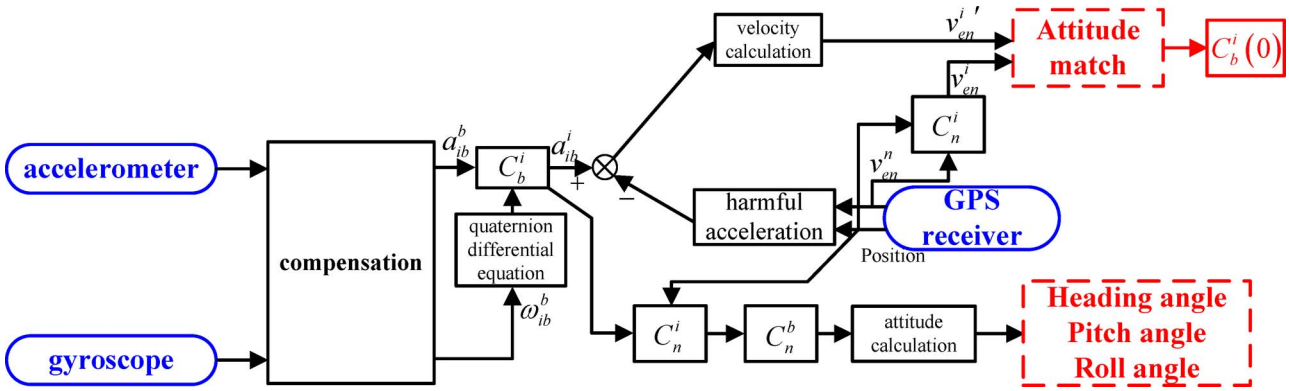

Fig. 3. Signal flow graph (strapdown flow after modification).

where $\lambda(t)$ denotes longitude, $L(t)$ denotes latitude, and $h(t)$ denotes altitude.

The other two variables $v_{en}^n(\tau)$ and $\omega_{en}^n(\tau)$ can be substituted by GPS velocity information.

After the modification of the strapdown model, the information flow is changed into the form as the figure shown as below; all the feedback circles have been truncated so as to make parse resolution possible. In Fig. 3, the information from the GPS receiver is imported to substitute the intermediate quantity; therefore, with the velocity and position information, the velocity and position channels are truncated.

Thus, IFA is transformed into the "Wahba Problem" [18], [20], but there are two questions left.

1) The data rate is different between $\alpha(t)$ and $\beta(t)$;
2) The error involved by the substitution of the GPS information.

For question 1, as $\alpha(t)$ is calculated by IMU data, which are generally 100 or 200 Hz, and $\beta(t)$ is calculated by GPS data, which are generally 1 to 20 Hz, thus, sampling time points should be chosen according to the GPS data.

For question 2, the GPS position and velocity errors take effect in two terms of $\int_0^t C_n^i(\tau)((2C_i^n(\tau)\omega_{ie}^i + \omega_{en}^n(\tau)) \times v_{en}^n(\tau))d\tau$ and $\int_0^t C_n^i(\tau)g^n d\tau$; the influence of the two terms to the integral operation should be checked.

The GPS position error takes effect in term $C_n^i(\tau)$, within one GPS updating period (the frequency of the GPS in the POS is usually 10∼20 Hz); the error of $C_n^i(\tau)$ involved by the GPS position error is so small, which can be neglected.

The GPS velocity error takes effect in two terms, i.e., $C_n^i(\tau)(\omega_{en}^n(\tau) \times v_{en}^n(\tau))$ and $C_n^i(t)v_{en}^n(t)$, in $C_n^i(\tau)(\omega_{en}^n(\tau) \times v_{en}^n(\tau))$; as shown in the equation, the GPS velocity error is imported as the second-order small quantity. However, for the sake of high precision, it is still needed to take some methods to reduce the error as much as possible. Here, for efficiency and convenience, linear interpolation is involved to describe the samples within two GPS sample points. In $C_n^i(t)v_{en}^n(t)$, the influence will be analyzed in the latter sections.

Thus, the two aforementioned questions can be completely solved.

In theory, ideally, there exists one value of $C_b^i(0)$, which can be taken as the initial attitude matrix to make (10) identical at any time in the process of navigation; thus, to solve the IFA problem is just to get the optimal initial attitude matrix $C_b^i(0)$.

After the aforementioned modeling, the latter steps to get the optimal initial attitude matrix $C_b^i(0)$ are identical with the steps in [18], which is listed below for method integrity.

Accordingly, the operator is defined as

$$\begin{bmatrix} + \\ q_1 \end{bmatrix} \triangleq \begin{bmatrix} s_1 & -\eta_1^T \\ \eta_1 & s_1 I + (\eta_1 \times) \end{bmatrix} \triangleq \begin{bmatrix} - \\ q_2 \end{bmatrix} \triangleq \begin{bmatrix} s_2 & -\eta_2^T \\ \eta_2 & s_2 I - (\eta_2 \times) \end{bmatrix}. \tag{14}$$

Equation (10) can be transformed as

$$\left(\begin{bmatrix} + \\ \beta(t) \end{bmatrix} - \begin{bmatrix} - \\ \alpha(t) \end{bmatrix} \right) q = 0. \tag{15}$$

In (15), the optimal attitude quaternion q is subject to

$$\begin{aligned} \min_q \int_0^{t_f} \left\| \left(\begin{bmatrix} + \\ \beta(t) \end{bmatrix} - \begin{bmatrix} - \\ \alpha(t) \end{bmatrix} \right) q \right\|^2 dt \\ = \min_q q^T \int_0^{t_f} \left(\begin{bmatrix} + \\ \beta(t) \end{bmatrix} - \begin{bmatrix} - \\ \alpha(t) \end{bmatrix} \right)^T \\ \times \left(\begin{bmatrix} + \\ \beta(t) \end{bmatrix} - \begin{bmatrix} - \\ \alpha(t) \end{bmatrix} \right) dt q. \end{aligned} \tag{16}$$

Here, define

$$K = \int_0^{t_f} \left(\begin{bmatrix} + \\ \beta(t) \end{bmatrix} - \begin{bmatrix} - \\ \alpha(t) \end{bmatrix} \right)^T \left(\begin{bmatrix} + \\ \beta(t) \end{bmatrix} - \begin{bmatrix} - \\ \alpha(t) \end{bmatrix} \right). \tag{17}$$

Thus

$$\min_q \int_0^{t_f} \left\| \left(\begin{bmatrix} + \\ \beta(t) \end{bmatrix} - \begin{bmatrix} - \\ \alpha(t) \end{bmatrix} \right) q \right\|^2 dt \triangleq \min_q q^T K q.$$

and q is subject to

$$q^T q = 1 \tag{18}$$

To make (18) come into existence naturally, with the LaGrange multiplier method, define

$$L(q) = q^T K q - \lambda(q^T q - 1). \tag{19}$$

Matrix K is subject to

$$(K + \lambda I)q = 0. \tag{20}$$

The smaller $L(q)$ is, the closer the INS navigation velocity vector is to the GPS velocity vector. The minimum eigenvalue $\lambda_{\min}$ of K is the minimum value that $L(q)$ can reach. Thus, when q is eigenvector $q_{\lambda_{\min}}$ with respect to the minimum eigenvalue $\lambda_{\min}$ of K, $L(q)$ reaches its minimum value $\lambda_{\min}$, and ideally, in theory, $\lambda_{\min}$ should be zero.

In ground static base alignment, with known velocity $v_{en}^n(t) \equiv 0$ substituting into (11), the proposed method in this paper can be transformed into the method in [18], which is essentially a special case of the proposed method in this paper.

III. Real-Time Implementation

The proposed algorithm can be applied in real-time circumstance with some necessary improvement; the specific is as follows.

Different from postprocessing, in real-time circumstance, the unknown amount to solve is the attitude at the current time t but not at the initial time t_0.

Supposing that the alignment result at time t is $C_b^i(t_0)$ with the algorithm in Section II, attitude C_b^n, which is focused at time t, is retrieved as

$$C_b^n(t) = C_e^n(t) C_i^e(t) \chi(t_0, t) C_b^i(t_0)$$

in which $C_e^n(t)$ and $C_i^e(t)$ are retrieved as in (13).

IV. Experiments

To evaluate the availability, the performance, and the accuracy of the proposed algorithm in real-time application, flight experiment is carried out.

In flight experiment, the newly designed POS by Beijing University of Aeronautics and Astronautics (BUAA) is used, in which the IMU consists of high-precision laser gyroscopes and accelerometers. The picture and the performance parameters are shown in Fig. 4 and Table I, respectively.

Fig. 4. POS (BUAA) used in the experiment.

TABLE I
Specifications of POS (BUAA)

Sensors	Specifications
IMU	Gyroscope: random constant <0.005°/h, white noise <0.01°/h. (1σ)
	Accelerometer: random constant <50ug, white noise <50ug. (1σ)
Differential GPS	Velocity: 0.05m/s (RMS)
	Position: 0.1m (RMS)

Fig. 5. Hardware configuration and flight experiment environment.

Flight Experiment

Aside from the car-mounted experiment, the flight experiment is also carried out. The identical POS is used as in the car-mounted experiment. The aircraft sketch map and the flight track are shown in Figs. 5 and 6, respectively.

As the aforementioned track shows, the alignment section is an "S" maneuver section, which lasts for about 400 s. In contrast, coarse alignment is implemented as well, as in car-mounted experiment with AEKF IFA. Because of airflow disturbance, the heading-angle error is about 15°, and the level attitude error is about 5°. In fine alignment process, because of the lack of *a priori* knowledge, the heading-angle uncertainty is set as 10°, and the level attitude uncertainty is set as 3°. The alignment result in real time is shown in Fig. 7.

The flight track as aforementioned is a section of an "S" maneuver; the alignment results of the two algorithms are (the alignment process is the same as in the car-mounted experiment) given in Fig. 7. What is needed to illuminate is that the heading error of the coarse alignment is about 30° as a result of the high speed of the wind; the level attitude error is about 5° as a result of airflow disturbance.

The whole process lasts for about 400 s as aforementioned; three sections are chosen to examine the converging time and the alignment attitude error.

The first section of alignment is the alignment result of the former 50 s (see Fig. 8); it is obvious that the attitude converges fast. In 30 s, the heading-angle error has converged to less than 0.5°, and the level attitude error has converged to less than 0.02°. In contrast, with AEKF IFA, the heading-angle error

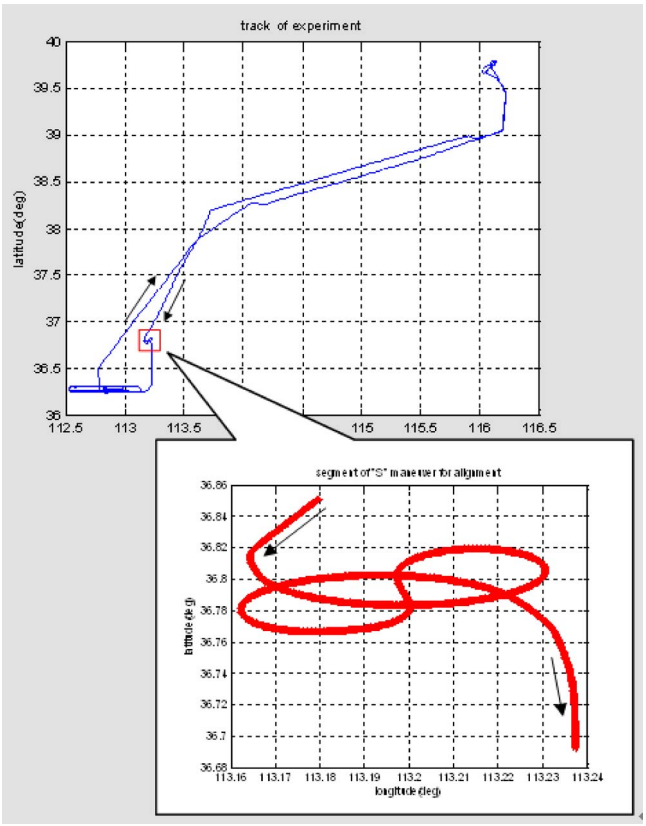

Fig. 6. Flight track and the section for IFA.

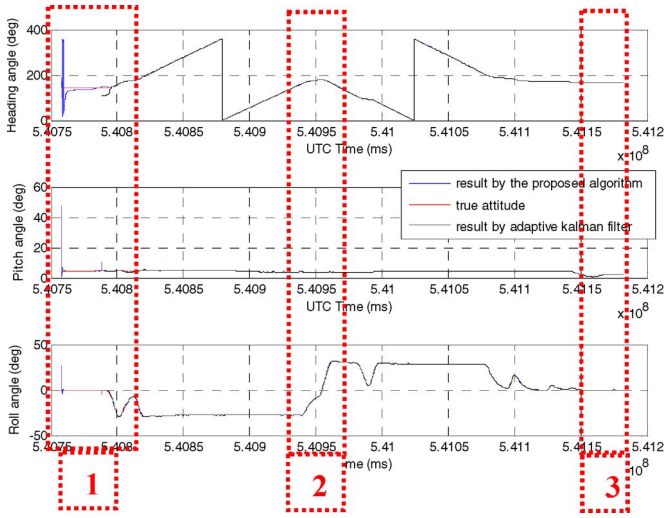

Fig. 7. Alignment result.

has converged to less than 0.6°, and the level attitude error has converged to less than 0.05°.

The second section of alignment is the alignment result after about 200 s (see Fig. 9); the heading-angle error has converged to less than 0.02°, and the level attitude error has converged to less than 0.005°. In contrast, with AEKF IFA, the heading-angle error has converged to less than 0.07°, and the level attitude error has converged to less than 0.01°.

The third section of alignment is the alignment result in the end of 400 s (see Fig. 10). The alignment accuracy of the two algorithms are basically the same; the heading-angle error has

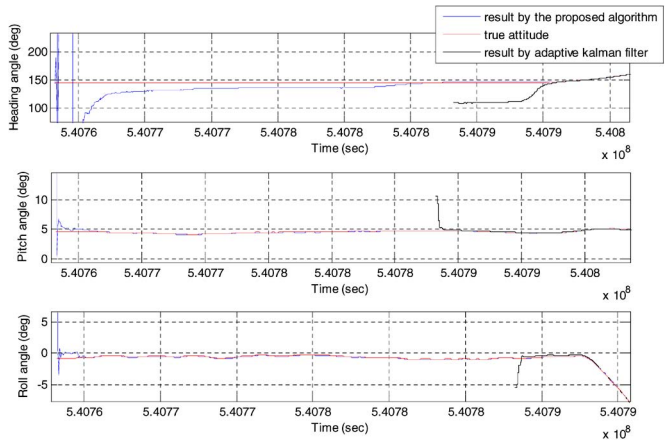

Fig. 8. Alignment result (the first section).

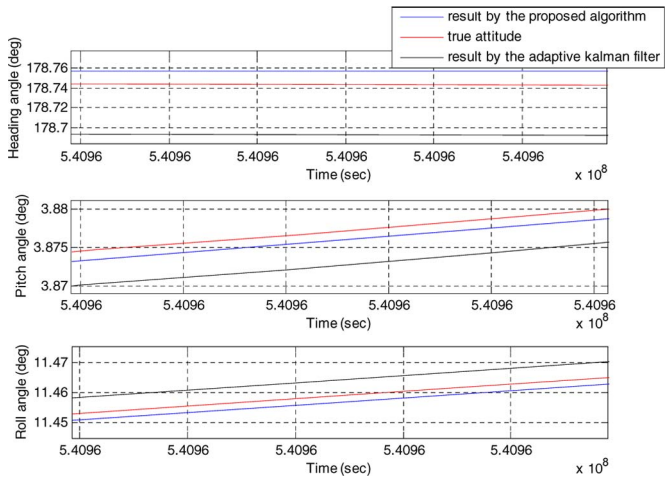

Fig. 9. Alignment result (the second position).

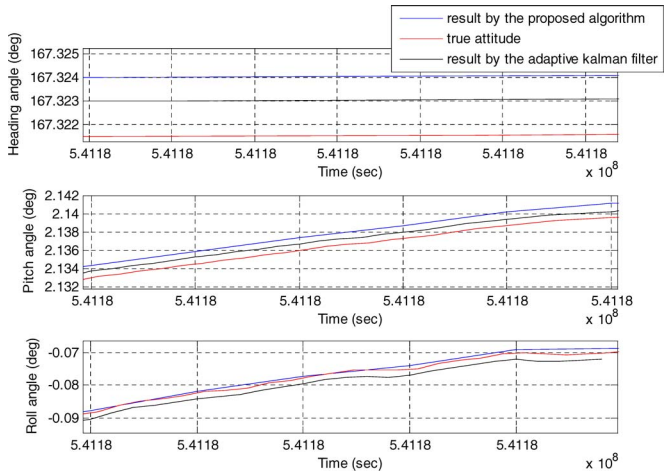

Fig. 10. Alignment result (the third position).

converged to less than 0.003°, and the level attitude error has converged to less than 0.002°.

Different from the car-mounted experiments, the "S" maneuver can be implemented in the process of flight; in this process, the heading angle can converge toward the true value fast.

TABLE II
ALIGNMENT RESULT (100 S)

	Heading Angle (deg)	Pitch angle (deg)	Roll angle (deg)
Result by the proposed algorithm	271.7656	4.8186	-27.8803
Result by AEKF IFA	271.5759	4.8518	-27.9117
True attitude (Post-process result of POS)	271.6841	4.8312	-27.8927
Attitude error of the proposed algorithm	0.0815	-0.0126	0.0124
Attitude error of AEKF IFA	-0.1082	0.0206	-0.0190

TABLE III
COMPARING IN CONVERGING TIME

	Heading Angle (s)	Pitch angle (s)	Roll angle (s)
Attitude error of the proposed algorithm	72.04	5.25	10.62
Attitude error of AEKF IFA	103.87	55.41	35.98

The respective alignment result error after 100 s is shown in Table II.

Examine the convergence time of both of the two algorithms, within which the heading-angle error gets less than 0.1° and the level attitude error gets less than 0.02°; the result is shown in Table III.

We notice that the alignment result of the proposed algorithm converges much faster than AEKF IFA.

V. CONCLUSION

This paper has devised a novel IFA method based on the equivalent q-method to the Wahba problem, which transforms the IFA problem into a quaternion optimization problem by finding the minimum eigenvector. Meanwhile, in the static state, the proposed algorithm can be transformed into the algorithm in [18], which can be therefore considered a special case of the proposed algorithm in this paper.

Experiments have clearly demonstrated that the proposed algorithm converges faster and is more robust than AEKF IFA. Meanwhile, it has no restrictions on maneuver.

REFERENCES

[1] M. M. R. Mostafa and J. Hutton, "Direct positioning and orientation systems how do they work? What is the attainable accuracy?" in *Proc. Amer. Soc. Photogramm. Remote Sens. Annu. Meeting*, 2001, pp. 17–11.

[2] F. Jiancheng and Y. Sheng, "Study on innovation adaptive EKF for in-flight alignment of airborne POS," *IEEE Trans. Instrum. Meas.*, vol. 60, no. 4, pp. 1378–1388, Apr. 2011.

[3] D. H. Titterton and J. L. Weston, *Strapdown Inertial Navigation Technology*. Herts, U.K.: IEE, 2004.

[4] G. Xiaolin, "Research on the filtering methods and experiments of SINS/GPS for imaging of airborne Earth observation," Ph.D. dissertation, Beihang Univ., Beijing, China, May 2009.

[5] F. Jiancheng and G. Xiaolin, "Predictive iterated Kalman filter for INS/GPS integration and its application to SAR motion compensation," *IEEE Trans. Instrum. Meas.*, vol. 59, no. 4, pp. 909–915, Apr. 2010.

[6] X. Gong and J. Fang, "Analyses and comparisons of some nonlinear Kalman filters in POS for airborne SAR motion compensation," in *Proc. IEEE Int. Conf. Mechatron. Autom.*, Harbin, China, 2007, pp. 1495–1500.

[7] S. P. Dmitriyev and O. A. Stepanov, "Nonlinear filtering methods application in INS alignment," *IEEE Trans. Aerosp. Electron. Syst.*, vol. 33, no. 1, pp. 260–272, Jan. 1997.

[8] H. S. Hong, C. G. Park, and J. G. Lee, "A leveling algorithm for an underwater vehicle using extended Kalman filter," in *Proc. IEEE Position Location Navig. Symp.*, Palm Springs, CA, 1998, pp. 280–285.

[9] K. J. Kim and C. G. Park, "in-flight alignment algorithm based on nonsymmetric unscented transformation," in *Proc. SICE-ICASE Int. Joint Conf.*, Busan, Korea, 2006, pp. 4916–4920.

[10] J. Yang, H. Y. Zhang, and J. Li, "INS nonlinear alignment with large azimuth misalignment angle using predictive filter," *J. Chin. Inertial Technol.*, vol. 11, no. 6, pp. 44–52, Dec. 2003.

[11] A. S. Jurkov, J. Cloutier, E. Pecht, and M. P. Mintchev, "Experimental feasibility of the in-drilling alignment method for inertial navigation in measurement-while-drilling," *IEEE Trans. Instrum. Meas.*, vol. 60, no. 3, pp. 1080–1090, Mar. 2011.

[12] A. R. Jimenez Ruiz, "Accurate pedestrian indoor navigation by tightly coupling foot-mounted IMU and RFID measurements," *IEEE Trans. Instrum. Meas.*, vol. 61, no. 1, pp. 178–189, Jan. 2012.

[13] E. Pecht and M. P. Mintchev, "Observability analysis for INS alignment in horizontal drilling," *IEEE Trans. Instrum. Meas.*, vol. 56, no. 5, pp. 1935–1945, Oct. 2007.

[14] N. El-Sheimy, K.-W. Chiang, and A. Noureldin, "The utilization of artificial neural networks for multisensor system integration in navigation and positioning instruments," *IEEE Trans. Instrum. Meas.*, vol. 55, no. 5, pp. 1606–1615, Oct. 2006.

[15] J. J. Simon and J. K. Uhlmann, "Unscented filtering and nonlinear estimation," *Proc. IEEE*, vol. 92, no. 3, pp. 401–422, Mar. 2004.

[16] T. M. Pham, "Kalman filter mechanization for INS airstart," in *Proc. Digit. Avionics Syst. Conf.*, Los Angeles, CA, Oct. 1991, pp. 516–525.

[17] B. M. Scherzinger and D. B. Reid, "Inertial navigation error models for large heading uncertainty," in *Proc. IEEE Position, Location Navig. Symp.*, Atlanta, GA, 1996, pp. 477–484.

[18] M. Wu, Y. Wu, X. Hu, and D. Hu, "Optimization-based alignment for inertial navigation systems: Theory and algorithm," *Aerosp. Sci. Technol.*, vol. 15, no. 1, pp. 1–17, Jan./Feb. 2011.

[19] Y. Wu, M. Wu, X. Hu, and D. Hu, "Self-calibration for land navigation using inertial sensors and odometer: Observability analysis," in *Proc. AIAA Guidance, Navig. Control Conf.*, Chicago, IL, 2009, pp. 10–13.

[20] G. Wahba, "A least squares estimate of spacecraft attitude," *SIAM Rev.*, vol. 7, no. 3, p. 409, Jul. 1965.

[21] I. Rhee, M. F. Abdel-Hafez, and J. L. Speyer, "Observability of an integrated GPS/INS during maneuvers," *IEEE Trans. Aerosp. Electron. Syst.*, vol. 40, no. 2, pp. 526–535, Apr. 2004.

[22] I. Y. Bar-Itzhack, "Minimal order time sharing filters for INS in-flight alignment," *J. Guid., Control, Dyn.*, vol. 5, no. 4, pp. 396–402, Jul. 1982.

[23] I. Y. Bar-Itzhack and N. Bermant, "Control theoretic approach to inertial navigation systems," in *Proc. J. Guid., Control, Dyn.*, 1987, vol. 2, pp. 1442–1453.

[24] I. Y. Bar-Itzhack and B. Porat, "Azimuth observability enhancement during inertial navigation system in-flight alignment," *J. Guid., Control, Dyn.*, vol. 3, no. 4, pp. 337–344, Jul. 1980.

[25] Y. Tang, Y. Wu, and M. Wu, "INS/GPS integration: Global observability analysis," *IEEE Trans. Veh. Technol.*, vol. 58, no. 3, pp. 1129–1142, Mar. 2009.

[26] D. N. Vizireanu and S. V. Halunga, "Analytical formula for three points sinusoidal signals amplitude estimation errors," *Int. J. Electron.*, vol. 99, no. 1, pp. 149–151, Jan. 2012.

[27] D. N. Vizireanu and S. V. Halunga, "Single sine wave parameters estimation method based on four equally spaced samples," *Int. J. Electron.*, vol. 98, no. 7, pp. 941–948, Jul. 2011.

[28] D. N. Vizireanu, "A simple and precise real-time four point single sinusoid signals instantaneous frequency estimation method for portable DSP based instrumentation," *Measurement*, vol. 44, no. 2, pp. 500–502, Feb. 2011.

[29] D. N. Vizireanu, "Quantized sine signals estimation algorithm for portable DSP based instrumentation," *Int. J. Electron.*, vol. 96, no. 11, pp. 1175–1181, Nov. 2009.
[30] R. M. Udrea and D. N. Vizireanu, "Quantized multiple sinusoids signal estimation algorithm," *J. Instrum.*, vol. 3, pp. 1–7, Feb. 2008.

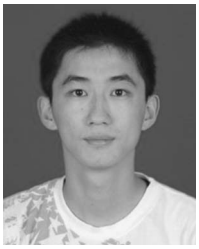

Kang Taizhong received the B.S. degree in 2007.

He is currently a Doctor with Beijing University of Aeronautics and Astronautics, Beijing, China, working within the field of inertial navigation and integrated navigation.

Fang Jiancheng received the Ph.D. degree from Southeast University, Nanjing, China.

He is currently a Professor with Beijing University of Aeronautics and Astronautics, Beijing, China, where he is also the Dean of the School of Instrumentation Science and Optoelectronics Engineering and the Director of the Key Laboratory of Fundamental Science for National Defense of Novel Inertial Instrument and Navigation System Technology. His research interests include design and error analysis of inertial sensor, navigation and attitude control of aerocraft, and optimal estimation theory.

Wang Wei, photograph and biography not available at the time of publication.